Stress-Localized Durable Anti-Biofouling Surfaces

Bahareh Eslami, Peyman Irajizad, Parham Jafari, Masoumeh Nazari, Ali Masoudi, Varun

Kashyap, Shane Stafslien[‡] and Hadi Ghasemi*[†]

[†]Department of Mechanical Engineering, University of Houston, 4726 Calhoun Rd, Houston,

Texas, 77204-4006, USA

‡Office of Research and Creative Activity, North Dakota State University, Fargo, North Dakota,

58102, USA

E-mail: hghasemi@uh.edu

Keywords: Stress-localization, anti-biofouling, adhesion, durability

Abstract

Growing demands for bio-friendly antifouling surfaces has stimulated development of new and

ever-improving material paradigms. Despite notable progress in bio-friendly coatings, the

biofouling problem remains a critical challenge. In addition to biofouling characteristics,

mechanically stressed surfaces such as ship hulls, piping systems, and heat exchangers require

long-term durability in marine environment. Here, we introduce a new generation of anti-

biofouling coatings with superior characteristics and high mechanical, chemical and

environmental durability. In these surfaces, we have implemented the new physics of stress-

localization to minimize adhesion of bio-species on the coatings. This polymeric material

1

contains dispersed organogels in a high shear modulus matrix. Interfacial cavitation induced at the interface of bio-species and organogels particles lead to stress-localization and detachment of bio-species from these surfaces with minimal shear stress. In a comprehensive study, the performance of these surfaces is assessed for both soft and hard-biofouling including Ulva, bacteria, diatoms, barnacles and mussels and is compared with state-of-the-art surfaces. These surfaces show Ulva accumulation of less than 1%, minimal bacteria biofilm growth, diatom attachment of 2%, barnacle adhesion of 0.02 MPa and mussel adhesion of 7.5 N. These surfaces promise a new physics-based route to address the biofouling problem and avoid adverse effect of biofouling on environment and relevant technologies.

INTRODUCTION

Biofouling is an outcome of undesired marine organisms' accumulating on surfaces. It impacts a variety of industries such as naval, heat exchangers, piping systems, and medical fields^{1–4} adversely. Any engineered structure immersed in water is prone to irreversible settlement of fouling organisms on it which leads to both economic and environmental penalties^{1,5}. Marine fouling on ship hulls increases the hydrodynamic drag resistant forces leading to lesser maneuverability of vessels and higher fuel consumption. This inevitably gives rise to emission of harmful compounds^{5–7}. Moreover, it accelerates surface corrosion, damage to protective coatings and required cleaning maintenance at a cost of billions of dollars a year to the maritime industry^{2,8}. The estimated cost due to fouling for the US Navy fleets, which represents only 1% of world fleets in numbers, is approximately \$200M per year^{1,6}. Hence, development of new materials to solve biofouling problem is of immediate importance.

Fouling process initiates with the formation of conditioning film induced by accumulation of physically adsorbed organic molecules (proteins, polysaccharides, glycoproteins) as a precursor to microfouling settlements, including bacteria, fungi, and protozoans^{9–12}. This colonization is governed by Brownian motion, electrostatic interactions and Van der Waal's forces^{13,14}. The growth development proceeds with macro-fouler establishments such as barnacles, mussels, hydroids, and tubeworms^{15,16}. The diversity of fouling organisms including their diverse adhesion mechanisms leads to complexity in design of anti-biofouling coatings¹. Fundamental understanding and manipulation of the adhesion mechanism and stability of the responsible forces of the adhesive complex to the substrate are paramount to develop highly efficient and reliable antifouling surfaces ^{17,18}. The progress of antifouling surfaces is attributed to modification of effective parameters such as topography^{19,20}, roughness²¹, surface energy^{22,23}, and elasticity modulus^{24,25}. Historically, toxic antifouling agents containing biocides such as lead, arsenic, mercury and their organic derivatives were used on ship hulls. Tributyltin (TBT), a revolutionary self-polishing copolymer was the most successful in combating bio-fouling in ships and was estimated to cover 70% of the world's fleet²⁶. However, its use was banned globally in 2008 by the International Maritime Organization (IMO) due to severe shellfish deformities and the bioaccumulation of tin in some ducks, seals and fish^{27–30}. Numerous investigations have been conducted to substitute the biocidal toxic surfaces with biocompatible fouling resistant coatings^{27,31} including silicone elastomer based materials⁹, fouling release paints^{1,32–35}, organogels^{36,37}, fluoropolymers³⁴, Poly (ethylene glycol)^{38,39}, slippery liquid-infused porous surfaces (SLIPS)⁴⁰⁻⁴⁴, Zwitterionic⁴⁵⁻⁴⁸, Polydimethylsiloxane-based materials^{49,50}, and bioinspired micro/nano topographical surfaces^{51–53}. The zwitterionic polymers have received increasing attention over the recent years for their promising ultralow fouling and antibacterial

properties. Surface hydration layer is the main antibacterial mechanism responsible for repelling the bacteria and fouling species. Strong hydrogen-bond of water molecules at the polymer surface and electrostatic interactions improve their performance. However, lack of long-term durability and mechanical stability have limited the effectiveness of theses anti-biofouling coatings. Various durability tests should be conducted to qualify antifouling surfaces for marine environment. It is also noteworthy that applicability of coating techniques in large scales is an essential parameter in the naval industry.

Here, we present a new generation of durable anti-biofouling materials called stress-localized surfaces. These surfaces are based on a new physics, stress-localization⁵⁴, developed to minimize adhesion of solids on a surface. This physics is implemented in stress-localized surfaces and their superior anti-biofouling performance is demonstrated. In a comprehensive assessment, adhesion of five different marine organisms is analyzed on these coatings. The performance of these stress-localized coatings was investigated in comparison with state-of-the-art silicone elastomer-based fouling-release coatings including Polydimethylsiloxane (PDMS), Silastic 2, polysiloxane and Intersleek 700. We demonstrated superior mechanical, chemical and environmental durability of these surfaces. Furthermore, on-site reparability of the coatings is demonstrated by spraying the coatings on the damaged area.

EXPERIMENTAL METHOD

1. Surface Development

The physics of stress-localization and mathematical derivations is discussed in our recent publication⁵⁴. These surfaces are composed of two phases: phase (I) with high shear modulus and phase (II) with low shear modulus, **Figure 1**. Phase I is an elastomer with high shear modulus and phase II is organogel particles consisting of tuned liquid organic phases entrapped within a

solid phase (three-dimensionally crosslinked gel network). The shear stress for detachment of a solid from elastomers (σ) is proportional to shear modulus of elastomers ($\sigma \propto \sqrt{G}$)⁵⁵. That is why gels with low shear modulus have minimal adhesion to solid objects. In the stress-localization concept, visualized in **Figure 2**, once a solid (which here is a bio-foul) attaches to the coating, at the solid-coating surface, we have two interfaces, solid-phase I and solid-phase II. If the solid is exposed to a shear rate, solid locally detaches from phase II as phase II has low shear modulus. The detachment of solid from phase II forms some cavities at the solid-coating surface as shown in **Figure 2b**. Note that imposed shear stress forms cavities at the coordinate of phase II. The cavities at the interface localize stress at the periphery of the cavities. This localized shear stress opens the cavity and leads to detachment of solid from the coating. The stress-localization effect at the interface can reduce the shear stress for detachment of solid from the substrate by an order of magnitude compared to a material with the same shear modulus. We could also predict the stress-localization effect through first-principles as discussed in our previous work⁵⁴.

As shown in **Figure 2a**, we visualized the stress-localization effect through a developed experimental setup. A glass prism is attached to a stress-localized surface. The interface of the glass and the stress-localized surface is visualized through a high-speed imaging camera and a microscope. As shown in **Figure 2b**, by a small shear force, the cavities are formed at the coordinates of phase II. The fringes show the growth of the cavities. The growth of these cavities leads to final detachment of solid from the stress-localized surface.

Through mathematical formulation of the problem, the adhesion on stress-localized surfaces is written as⁵⁶

$$\sigma_{\rm S} = g(\varphi_{\rm II}) \left(\frac{a}{l}\right) \sqrt{\frac{\overline{W_a} G_m}{h}} \tag{1}$$

where $g(\varphi_{II})$ denotes the stress-localization function, a and l are the geometrical parameters in the adhesion measurement setup (**Figure 2c**), $\varphi_{\rm II}$ is the volumetric fraction of phase II, $\overline{W_a}$ is the work of adhesion of the material, and G_m is the shear modulus of the material. The value of stress-localization function varies between 0 and 1. It is demonstrated that this function reduces adhesion of a solid on a surface by an order of magnitude (i.e. $g(\varphi_{II})=0.1$)⁵⁶. We should add that the stress-localization concept is fundamentally different than the variation of shear modulus (G_m) method^{24,25}. For a constant value of G_m , adhesion stress is minimized through $g(\varphi_{II})$. Here, we implemented the same concept in anti-biofouling surfaces. Phase I in these structures is silicon elastomer with tensile strength of 8 N/mm², Shore hardness A of 30, tear strength of 13.5 N/m. The procedure for development of the organogels are as follow: 10 mL of Sylgard 184 base was mixed with 1 mL of Sylgard 184 curing agent. 100 mL of an organic liquid (i.e. Polydimethylsilaxone) was added to this mixture. The solution was then vigorously mixed to obtain a homogeneous solution. The precursor sample was heated at 100 °C for 4 hrs in a petri dish. The final product is a non-syneresis organogel. Non-syneresis property of organogel comes from miscibility of silicone oil with PDMS before and after gelation⁵⁷. Once phase II was developed, it was crushed in the presence of silicon oil for 10 mins to avoid aggregation of gel particles. The solution was filtered to remove excess oil. The final product is a batch of gel particles with dimension in the range of 2-20 µm. The particles were mixed with the elastomer in a pre-defined concentration. The solution was diluted with a solvent, Hexamethyldisilaxane, to reduce viscosity for spraying on a surface. Developed samples of ABF 1, ABF 2, and ABF 3 consist of 50%, 33% and 25% of phase II, respectively.

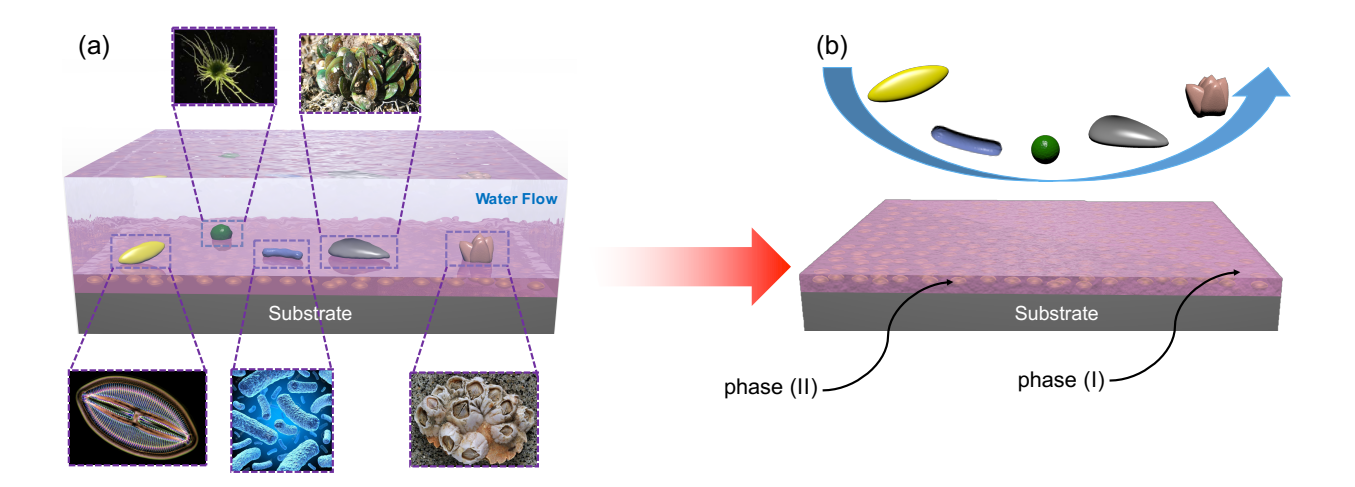


Figure 1. (a) and (b) Schematic of water flow including marine organisms (diatom *Navicula*, *Ulva* spores, bacterium, Mussels, and barnacles from left to right) over stress-localized coatings and its anti-biofouling property. The substrate formed of dispersed organogels (phase II) in a high shear modulus matrix (phase I).

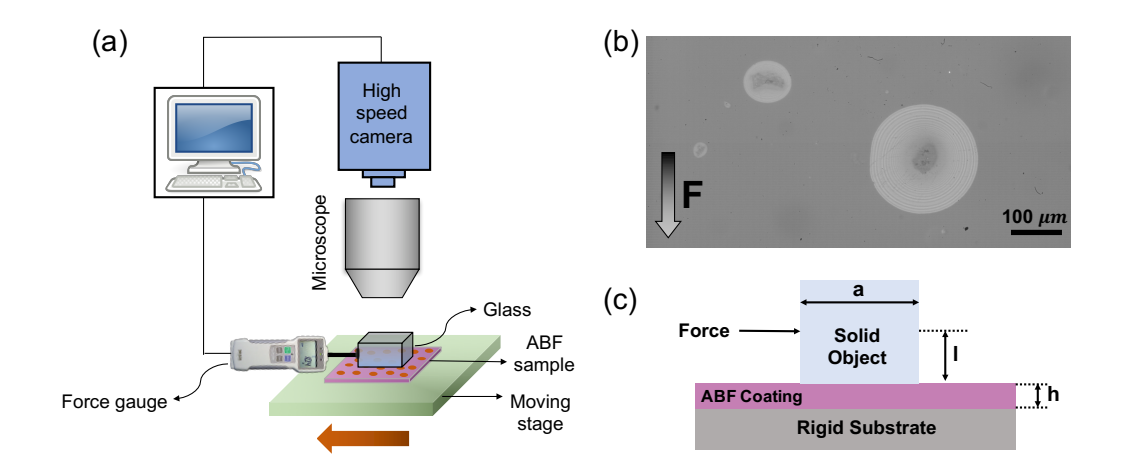


Figure 2. (a) Schematic of experimental setup to exhibit stress-localization mechanism using high-speed camera and microscope between glass and ABF substrate. (b) Interfacial cavities formed at phase II coordinate due to their low shear modulus. (c) The geometrical parameters in surface adhesion measurements.

2. Surface Characterization: Scanning Probe Microscopy (SPM, Bruker Multimedia 8) was used to characterize mechanical and surface properties of the anti-biofouling coatings and the

settled biological cells on the coating. SPM was set on ScanAsyst mode in air using Silicon Tip on Nitride cantilever. This mode allowed us to study adhesion behavior of the cells giving the information of preferred attachment coordinate and cell accumulation.

- **3. Biofouling Assays:** The studied fouling organisms belong to two main categories. They are 'microfouling' (i.e. *Ulva* spores, bacteria *Cytophaga lytica*, and diatom *Navicula*) and 'hard macrofouling' (i.e. barnacle and mussel). We utilized an environmental chamber (Carolina Biological Supply) to precisely control critical parameters such as light, humidity, and temperature to determine functionality of stress-localized coatings in the simulated marine environment.
- **3.1. Settlement of** *Ulva* **zoospores:** All the samples were placed in petri dishes and filled with the sea water solution containing suspended spores. To settle *Ulva* spores on the surface, the suspended spores were diluted to an absorbance of 0.15 at 660 nm and then added to the petri dishes. The petri dishes were transformed to the dark environmental chamber as quickly as possible and incubated at 20°C for 45-60 minutes⁵⁸. All the samples from each treatment were then washed 10 times by passing in a beaker of seawater to remove unsettled spores. To fix the settled cells on the substrates, an additional treatment was carried out by placing the samples inside 2.5% glutaraldehyde solution for 10-15 minutes.
- **3.2. Attachment and Adhesion of Bacterium** *C. lytica and* **Diatom** *Navicula*: Initial cell attachment and biofilm growth of algae were assessed before water jet adhesion analysis.

Bacterium C. lytica: A 5% suspension of bacterium in ASW + nutrients ($\sim 10^7$ cells.ml⁻¹) was prepared and 1 ml was added to each well of a 24 well-plate. A 24 well-plate was used to study characteristics of bio-species on the surface. The circular coupons were coated uniformly by ABF and other coatings with the same thickness of 100 μ m and were placed in the wells. Plates

were incubated at 28 °C for 24 hours to facilitate bacterial attachment and colonization. Then, plates were rinsed three times with DI water and stained with crystal violet. Images for analysis were taken after staining and extraction of crystal violet in 33% acetic acid (AA). The resulting eluates were measured for absorbance at 600 nm. After 24 hrs of bacteria settlement, water jet adhesion was conducted for 5 seconds at pressure of 10 and 20 psi (i.e. 69 and 138 kPa).

Diatoms Navicula: Diatoms were diluted to an optical density (OD) of 0.03 at 660 nm in artificial sea water (ASW) supplemented with nutrients. 1 ml of the diatom solution was added to each well and allowed to incubate in static condition for 2 hours to facilitate cell attachment. For biofilm growth analysis, the wells were incubated for 48 hours. Cell attachment and biofilm growth were quantified by fluorescence measurements of dimethylsulfoxide (DMSO) extracts of chlorophyll. Cell attachment/solution growth was reported as fluorescence intensity (relative fluorescence units). After 2 hrs of cell attachment, water jet adhesion was carried out for 10 seconds at pressure of 10 and 20 psi.

- **3.3.** Attachment and Adhesion of Hard Macrofouling Barnacle and Mussel: To examine attachment and adhesion of barnacles, six *A. amphitrite* barnacles were immobilized on the surface of the coatings. Coatings were analyzed after 2 weeks of reattachment with daily feedings of brine shrimp. In order to investigate adhesion behavior of mussel *Geukensia demissa*, coatings were analyzed after 3 days of attachment with two feedings of phytoplankton. A tensile force gauge, mounted to an automated stage, was used to measure the force required to completely remove attached barnacles and mussels from the surfaces.
- **4. Statistical Analysis:** The coverage percentage of species on the surfaces was measured through statistical analysis of images obtained from the fluorescence microscopy. To precisely excite and capture each species in fluorescence microscope, filters with different excitation and

emission spectra were utilized.

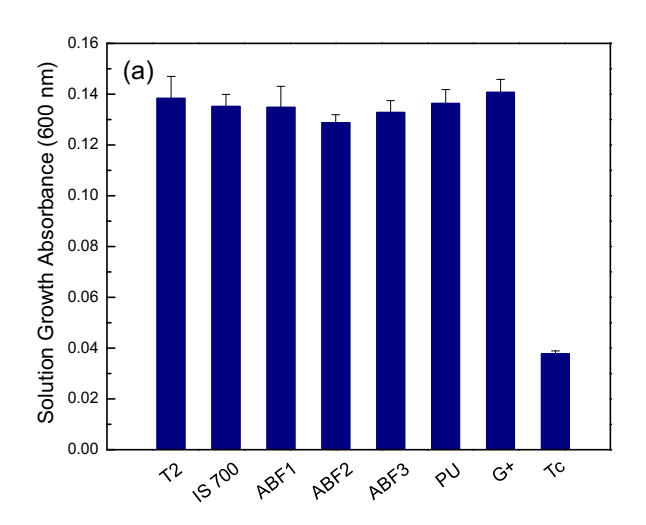
RESULTS AND DISCUSSION

Characteristics of Stress-Localized Anti-Biofouling (ABF) coatings:

Bio-friendly characteristics: These analyses were conducted after 14 days of water immersion preconditioning.

Leachate toxicity for *C. lytica* was assessed by introducing the bacterium into overnight extracts (artificial sea water with nutrients) for each coating and evaluating growth after 24 hrs via crystal violet colorimetric assay. Growth in coating leachates was reported as an absorbance ratio (600 nm) to a growth control. A series of negative growth controls (medium + bacteria + triclosan (Tc)) and positive growth control (G+) were also included in the analysis. The results are shown in **Figure 3a**. All the ABF coatings and other control samples show no toxicity.

Leachate toxicity for diatoms was assessed by introducing the microalgae into overnight extracts (artificial sea water with nutrients) for each coating. Growth evaluation was measured after 48 hours via fluorescence of chlorophyll and reported as a fluorescence ratio to a positive growth control (fresh nutrient medium). A negative growth control (medium + bacteria + triclosan) was also included in the analysis. The results are shown in **Figure 3b**. Similar to *C. lytica*, no toxicity was observed for all the samples.



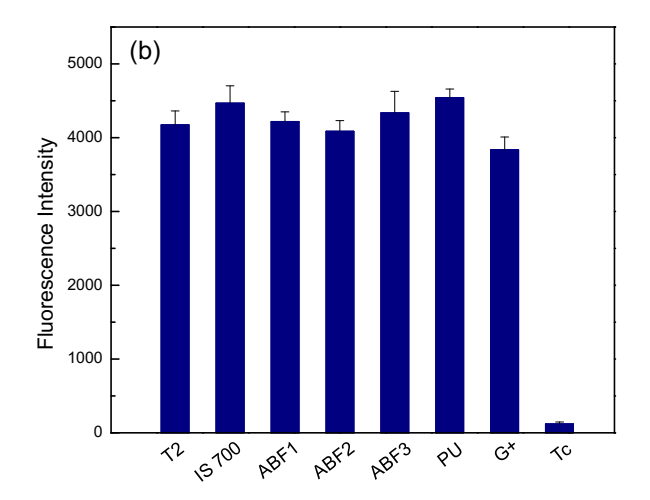


Figure 3. Assessment of leachate toxicity of ABF coatings and state-of-the-art coatings for (a) bacterium *C. lytica* after 24 hrs, and (b) diatom *Navicula* after 48 hrs. G+ and Tc are representatives of positive and negative growth control solutions, respectively. Error bars represent one standard deviation of the mean.

Ulva Attachment: Fouling formation is an outcome of the initial attachment of swimming *Ulva* zoospores to a suitable surface which forms sporelings adhesion consequently.⁵⁹ Once settled, the spores start to secrete the adhesive extracellular matrices which is a polydisperse, self-aggregating hydrophilic glycoprotein. They then undergo cross-linking with a corresponding rise in adhesion strength^{60,61}. Mechanical properties of secreted adhesive and surface properties of *Ulva* spores is studied through SPM. **Figure 4a** shows morphology of the spores on the surface and how they settle down on the substrate. For Ulva attachment, glycoprotein acts as an adhesive matrix (similar to EPS in diatoms attachment) and keeps the cell in contact with the surface which will be explained in more detail later⁶². In SPM, adhesion is characterized by pull-off force which measures adhesion between cantilever and substrate⁶³. Adhesion work is defined as pull-off force divided by the tip radius⁶³. As shown in **Figure 4b**, the highest adhesion belongs to glycoprotein formed around the cell. **Figure 4c** and **4d** depict SPM cantilever deformation and modulus of elasticity of spores, respectively. By comparing **Figure 4c** and **4d**, dependence of the

cantilever deformation on the modulus of elasticity is evident. The regions with highest elasticity show lowest cantilever deformation. The anti-biofouling property of stress-localized coatings is compared with PDMS in **Figure 4e-4f**. As shown, the stress-localized surface shows remarkable reduction in concentration of Ulva on the surface compared to PDMS. Statistical analysis of the fluorescence microscopy images reveals the concentration of *Ulva* spores on a surface in terms of percentage of colony coverage area. The analysis shows concentration of 8% for PDMS sample, while this value reduces to less than 1% (0.9 %) for ABF.

As discussed in the literature^{64,59}, low modulus of elasticity and critical surface tension are major determinants to low adhesion of spores and sporelings. However, low modulus of elasticity leads to poor mechanical durability of the coatings. Here, through the idea of stress-localization, we have achieved both low adhesion of spores on the surface and high mechanical durability.

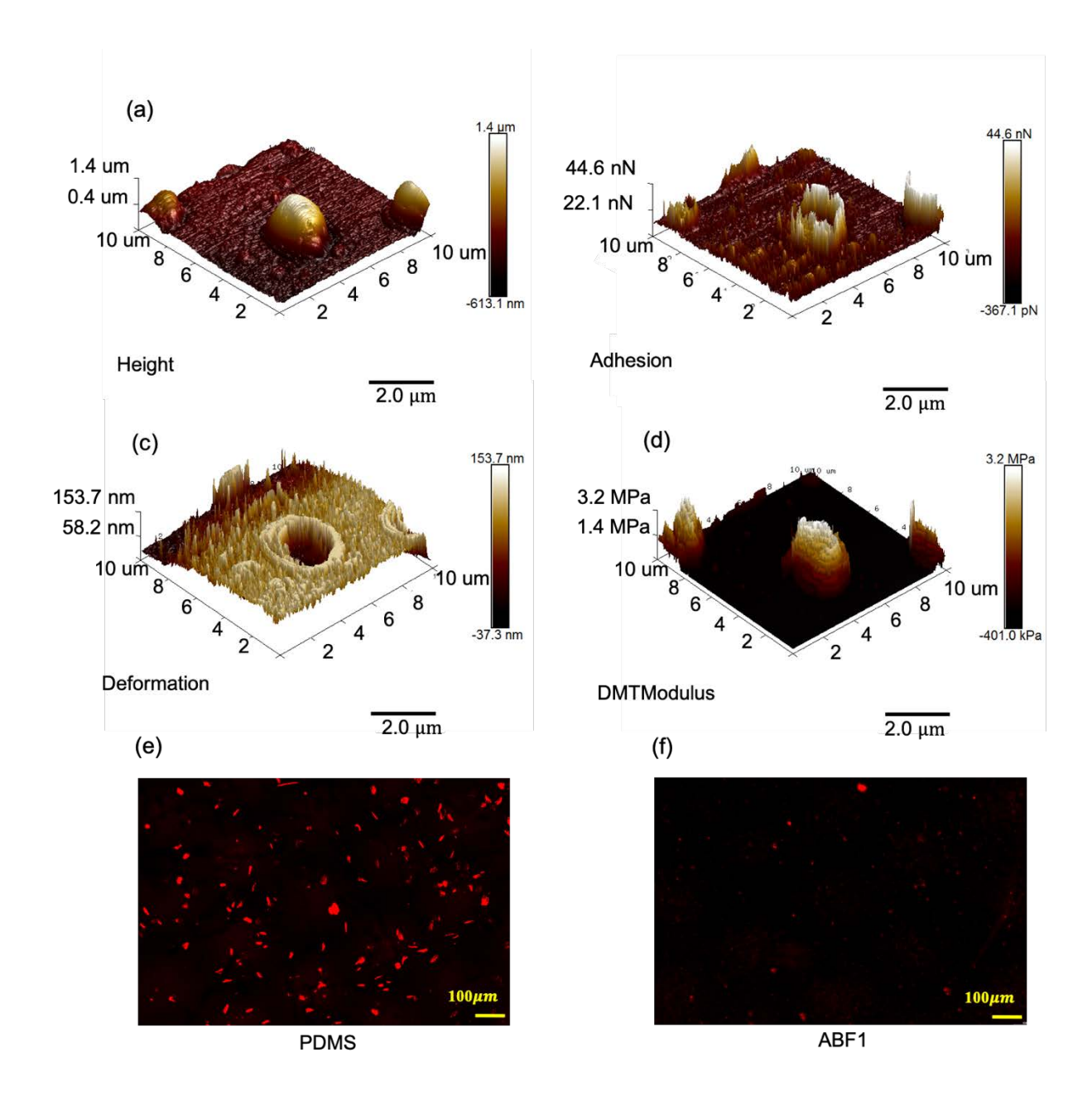


Figure 4. SPM analysis of *Ulva* on ABF coating showing (a) height graph, (b) adhesion, (c) deformation, and (d) elasticity modulus. Ulva spores attachment has been compared between (e) PDMS control sample and (f) ABF1.

Attachment and Adhesion of Marine Bacterium, *C. lytica*: Bacterium *C. lytica* as a component of microbial biofilm provides cues for settlement of other organisms on man-made structures⁶⁵. The results from the experimental assessment of biofilm growth and bacterium

attachment are illustrated in **Figure 5**. Biofilm growth was reported as the mean absorbance value of three replicate samples after 24 hours in **Figure 5a**. All the ABF coatings demonstrate smaller bacterial biofilm growth compared with state-of-the-arts. In the following step, the covered area was measured as presented in **Figure 5b** indicating the best result for ABF3, which is almost 20% less than Intersleek 700. **Figure 5c** shows the coated surfaces partially covered by bacterium *C. lytica*.

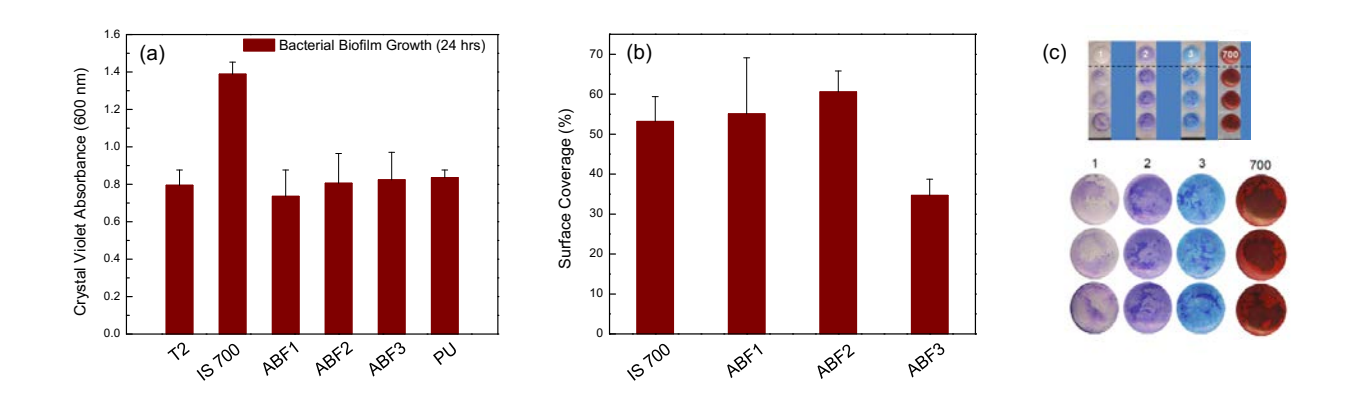
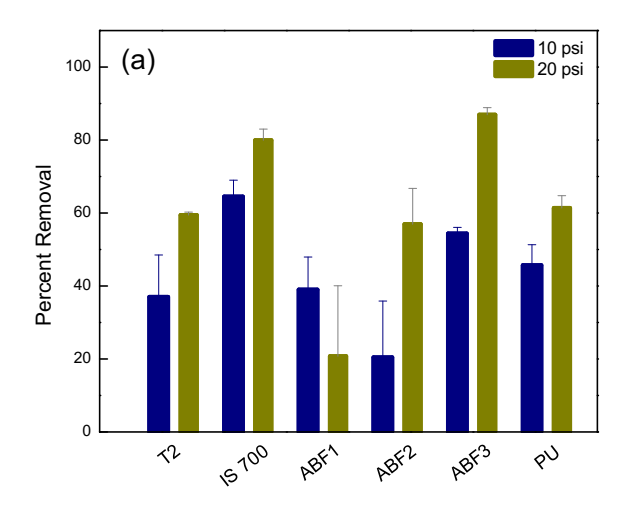


Figure 5. (a) Bacterial biofilm growth after 24 hours for ABF coatings in comparison with Silastic T2, Intersleek 700, and Polyurethane (PU). (b) Comparison of surface coverage for ABF coatings and Intersleek 700. (c) Graphical representation of bacterial attachment on the coatings.

Water jet adhesion was carried out after 24 hours of bacterial biofilm growth. The first column of each plate was not treated and served as the measure of biofilm growth before water jetting. The second and third columns of each stress-localized ABF coating were jetted for 5 seconds at a pressure of 10 psi and 20 psi, respectively. Biofilm adhesion was reported as a function of percent removal, **Figure 6a**, and remained biomass measured by colorimetric method via crystal violet absorbance, **Figure 6b**. Based on the results, ABF3 possesses highest removal percentage as well as the lowest remained biomass.



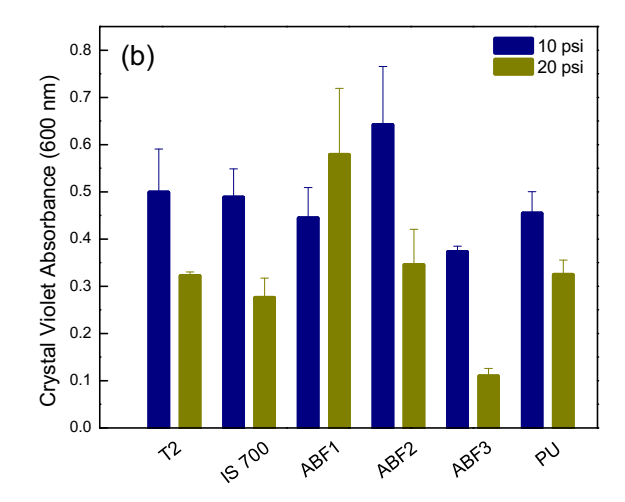


Figure 6. (a) Biofilm removal by exposing to water jet for two different pressures of 10 psi and 20 psi. (b) Remained biomass after exposure to water jet for two different pressures of 10 and 20 psi. T2 and PU stands for Silastic and Polyurethane, respectively. Error bars represent one standard deviation of the mean.

Attachment and Adhesion of Diatom *Navicula*: The motility of the diatoms in contact with a surface enable them to migrate and find the most suitable coordinate for settlement^{66,67}. Coordinate selection is not random but highly strategic and is based on diatom's potential to search for existing stalks. As diatoms seek out to find a proper coordinate, they secrete adhesive material called extracellular polymeric substances (EPS)^{9,68,69}. This material acts as a bridge between raphe and surface which results in deposition of a trail on the surface⁷⁰ and holds diatoms on the surface⁷¹. EPS is divided into two forms: bound EPS including tightly bound (TB) and loosely bound (LB), and soluble EPS. The bound EPS forms closely to the diatom and strongly bonds to it. The soluble EPS is weakly bonded to diatom and dissolves in the fluid environment⁷². Due to preference of diatoms for agglomeration, diatoms form a raft which constitutes of each individual EPS.⁶⁶ The SPM study in **Figure 7a** confirms this structure for EPS around the diatoms and both tightly bound and loosely bound EPS are highlighted . **Figure**

7b shows the deformation graph which is a representative of the SPM cantilever indentation. The highest deflection of cantilever occurs for the softest material which is EPS in this case. Less deformation can be seen for diatom due to its hard silica shield^{73,74}. Figure 7c represents the maximum adhesion for EPS and also shows the deposition of adhesive complex further away from the diatom on the surface. Figure 7d shows high modulus of elasticity of diatom compared to its surrounding. We analyzed the concentration of diatoms on the substrates through florescence microscopy. The results for PDMS and ABF3 sample are shown in Figures 7e and 7f. As shown, the superior anti-biofouling characteristics of ABF coatings are evident. The concentration of diatoms on PDMS sample is 20 %, while this value for ABF3 coating is 2% indicating an order of magnitude drop in diatom accumulation. Diatom attachment and biofilm growth are shown in Figure 8. All the ABF coatings have almost the same order of diatom attachment similar to Intesleek 700, Silastic T2, and PU.

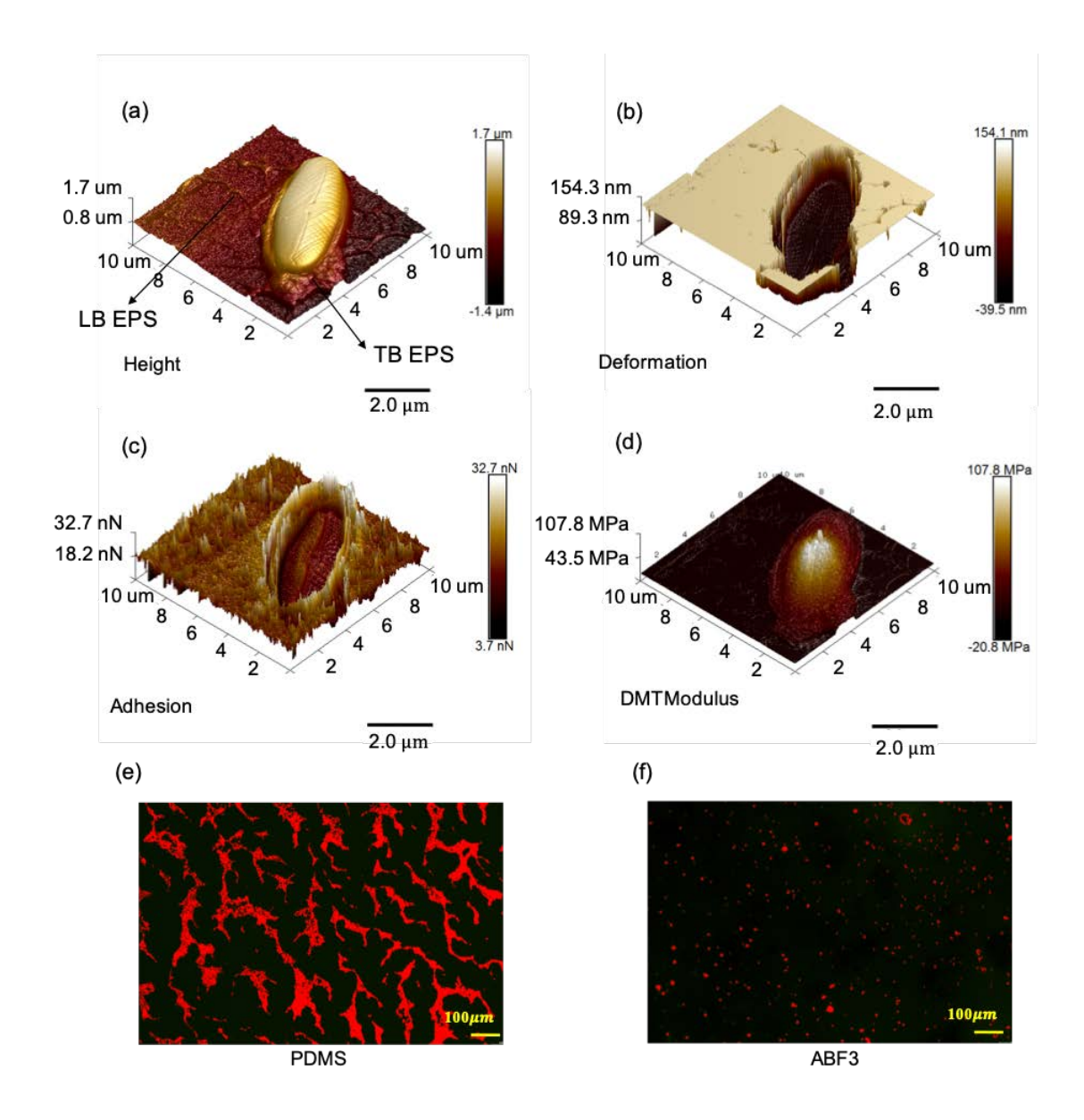


Figure 7. Diatom attachment and EPS formation on the surface of ABF3. (a) Tightly bound EPS is formed around the diatom and loosely bound EPS dispersed on the surface further away from diatom. (b) Deformation, (c) adhesion, and (d) modulus of elasticity of diatom and EPS. Highest deformation and adhesion is observed for EPS due to their sticky and soft nature. Diatom attachment has been compared between (e) PDMS control sample and (f) ABF3.

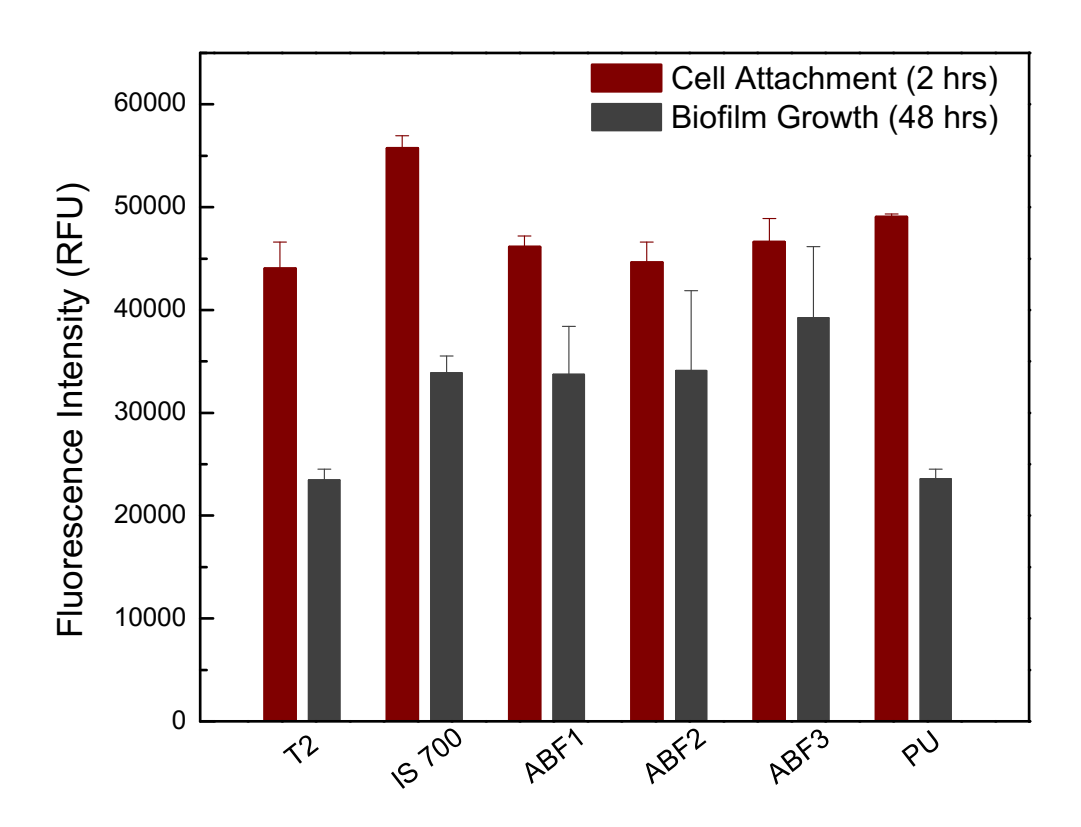
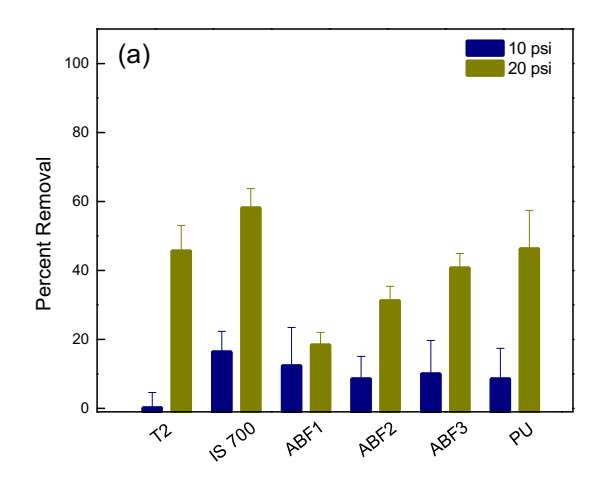


Figure 8. Diatom attachment measured after 2 hours and biofilm growth after 48 hours of incubation. The fluorescence values present concentration of diatoms attached to the coatings and biofilm growth on the surface. Error bars represent one standard deviation of the mean.

Water jet adhesion was conducted after 2 hours of initial cell attachment. The first column of each plate was not treated and served as the measure of cell attachment after 2 hours. The second and third column of each coating were jetted for 10 seconds at a pressure of 10 psi and 20 psi, respectively. Diatom adhesion was reported as a function of percentage removal, **Figure 9a**, and remained biomass measured by Fluorescence microscopy, **Figure 9b**. For 10 psi pressure, all the samples show the same performance. However, for 20 psi, Intersleek 700 shows slightly better performance than ABF samples.



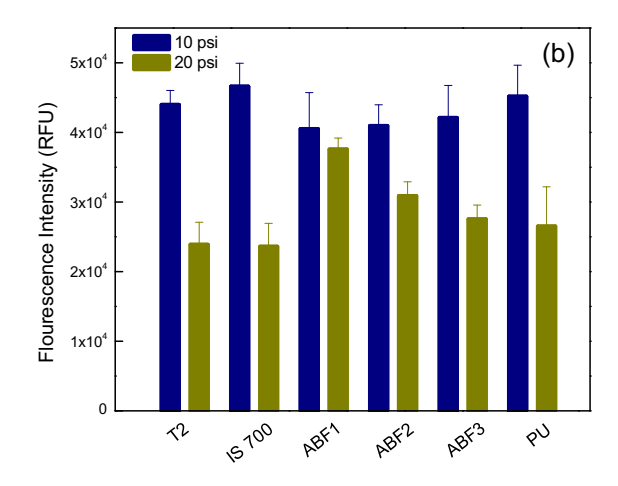


Figure 9. (a) Diatom *Navicula* removal by exposing to water jet for 10 seconds for two different pressures of 10 psi and 20 psi. (b) Remained biomass after exposure to water jet. Error bars represent one standard deviation of the mean.

Attachment and Adhesion of Barnacle: Barnacle is among the most common marine fouling organisms that has received considerable attention due to its strong and durable adhesive behaviour^{75,76}. This specie goes through six developmental stages starting from nauplii to adult cypris stage⁷⁷. Similar to other marine organisms, barnacle is able to sense a wide range of physical and chemical surface parameters to find the most suitable coordinate for settlement⁷⁷. By secreting proteinaceous cement from the cement gland, barnacle produces strong adhesion after going through several functions including establishment of interfacial contact and molecular attraction between dissimilar materials^{78,79}. Coatings were analyzed after 2 weeks of reattachment with daily feedings of brine shrimp. The number of barnacles that were able to attach to each surface were recorded and then reattachment efficiency calculated as shown in Figure 10a. ABF2 possesses the lowest barnacle attachment. Adhesion strength of barnacles was calculated then by dividing the measured force required to remove the barnacle by the basal area and reported in MPa. Each data point is the mean value of the total number of barnacles that reattached to the coating surface as shown in Figure 10b. The small shear value required to

remove the barnacle from ABF1, grants the privilege of high removal percentage. Adhesion strength is also relatively low for ABF2 and ABF3 and no significant difference can be seen with Intersleek 700. PU was not considered for barnacle test in this study as the result reported by Galhenage *et al*³⁹ which is almost 0 within the accuracy of their measurements.

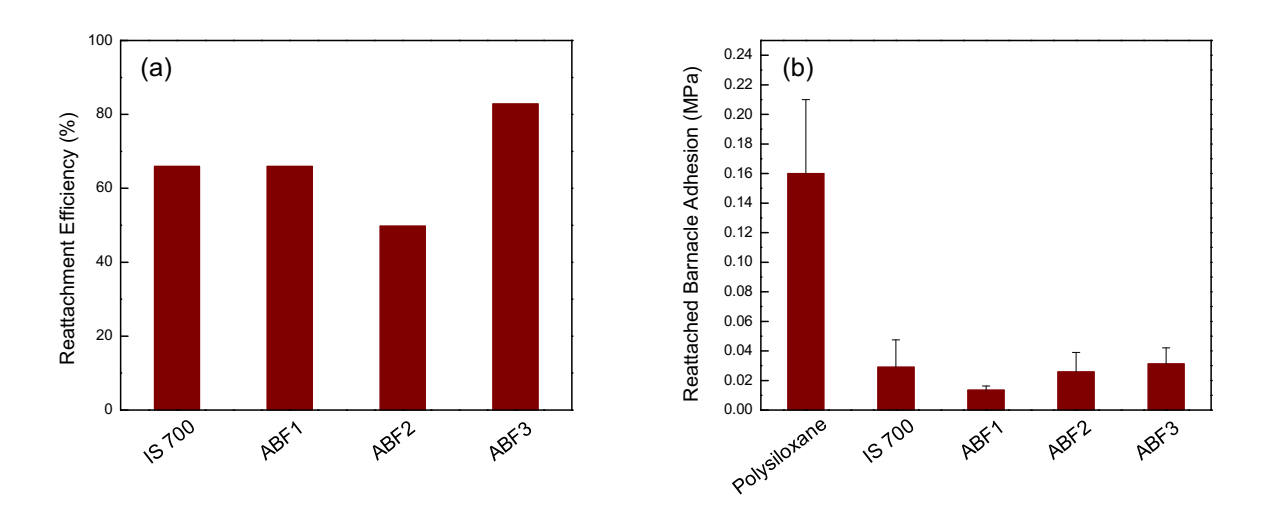
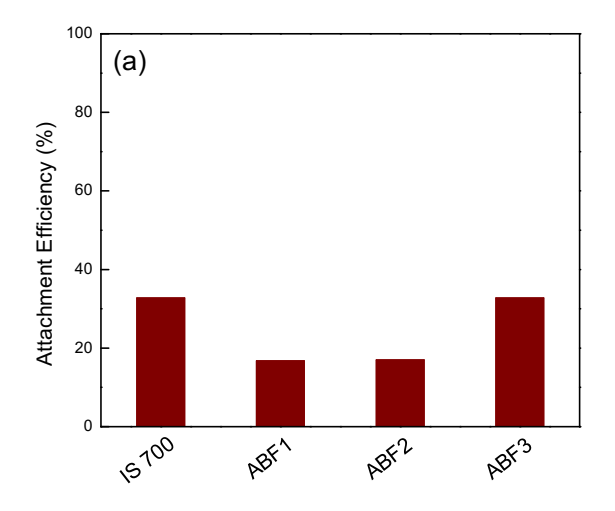


Figure 10. Assessment of barnacles (a) reattached efficiency after 2 weeks of daily feedings of brine shrimp, and (b) reattached adhesion on ABF (1, 2, and 3), Intersleek 700, and standard sample (polysiloxane) surfaces. Error bars represent one standard deviation of the mean.

Attachment and Adhesion of Mussel: Mussels attach to hydrophilic and hydrophobic solid surfaces via adhesive elastomeric protein based byssal threads⁴⁰. This special protein equips mussels to adhere to various surfaces including metals, minerals, plastics, cement, and even low surface energy fluoropolymers in their chemically heterogonous habbit⁸⁰. Their adhesion must be fast and strong to avoid them from getting dislodged and dashed by incoming waves⁸¹. Mussel *Geukensia demissa* was studied for its attachment and adhesion behavior. Coatings were analyzed after 3 days of attachment with two feedings of phytoplankton. Each data point is the mean value of all mussels that attached to the coating surface. The mean number of mussels settled on ABF1 and ABF2 are approximately half of Intersleek 700, illustrated in **Figure 11a**.

The required force for detachment of mussels from the surface was measured by using a tensile force gauge and minimum belongs to ABF1 (**Figure 11b**). PU was not tested for mussels in this study but result reported by Galhenage $et\ al^{39}$ which is 10 N.



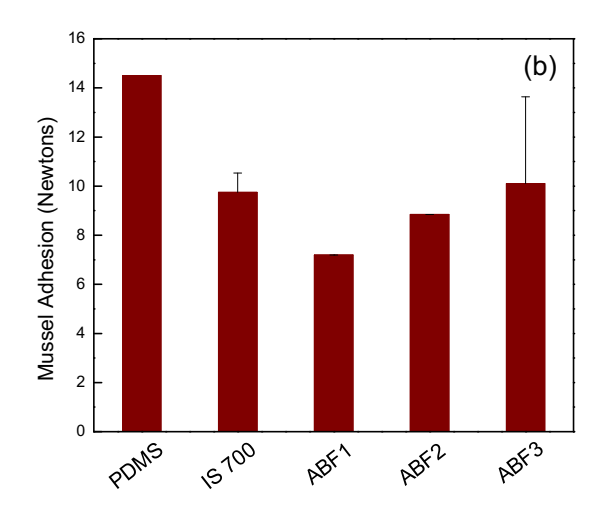


Figure 11. (a) Evaluation of mussel attachment on ABF (1, 2, and 3) and Intersleek coatings (700) after 3 days of feedings of phytoplankton. (b) Demonstrates the required adhesion to remove the mussels from the surface after measuring the attachment efficiency in part (a). Error bars represent one standard deviation of the mean.

Durability Test

We assessed mechanical, chemical and environmental durability of these surfaces. The mechanical durability was examined through abrasion of these surfaces by files and sands as shown in **Figure 12a**. The abrasion test was conducted using a Taber Reciprocating Abraser, model 5900 according to ASTM D4060. In this test, we measured material removal thickness at three different loading conditions (*i.e.* 1N, 5N, and 10 N) for 1000 abrasion cycles. Abrasion test results are presented in **Figure 13** for all three ABF coatings and standard PDMS. The primary thickness of each sample is 300 μ m. Minimum thickness loss belongs to ABF 3 which has the minimum percentage of organogels. The samples are durable with no sign of degradation in

response to mechanical stresses. For chemical durability, we immersed these samples in solutions with pH varying from 1.1 to 13.1 and kept the samples for a duration of 48 hrs in these solutions, **Figure 12b**. The anti-biofouling coatings show complete integrity with no sign of degradation. For environmental durability, the coated samples were examined according to ASTM G154. In this standard, the samples are exposed to 2000 hrs cycling. Each cycle includes 8 hrs exposure to UV-irradiation (0.49 W/m² nm at 310 nm at 70 °C) followed by 4 hrs of condensation at 50 °C. After this test, integrity of the coatings is examined to determine any surface defects on the surface. As shown in **Figure 12c**, the coatings are intact with no degradation. Finally, we demonstrated on-field reparability of these stress-localized coatings, **Figure 12d**. The coating was damaged by a sharp object and it is repaired through spraying of the new material. The sprayed material cures and integrates in the coating. This highlight facile implementation and application of these sprayable coatings compared to the other surface-modified approaches.

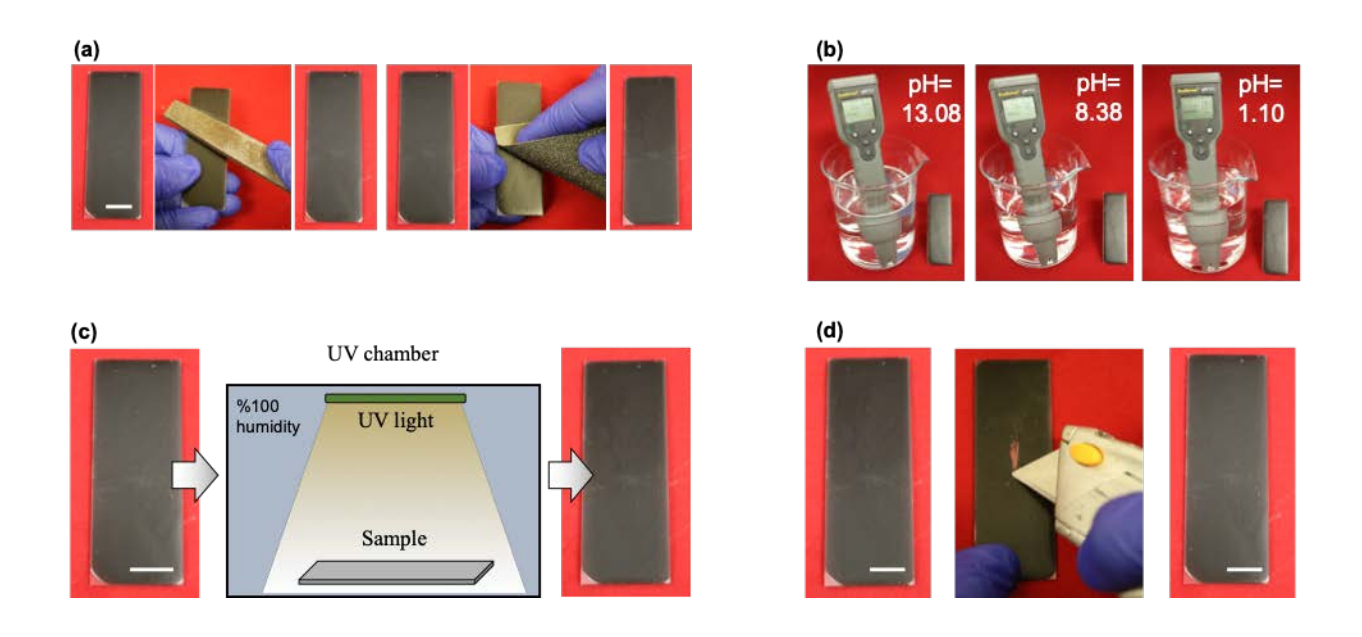


Figure 12. (a) Mechanical durability test of ABF3 (25% of phase (II)) by files and sands with no degradation in response to mechanical stresses. (b) Different range of pH from 1.1 to 13.1 for chemical durability test without any change in anti-biofouling performance of coatings. (c) The anti-biofouling surface was exposed to UV radiation for 2000 hours. No change in its performance was measured. (d) On-field reparability is demonstrated by removing some part of the material with a sharp blade and respraying of the material on the damaged area. The scale bar is 10 mm.

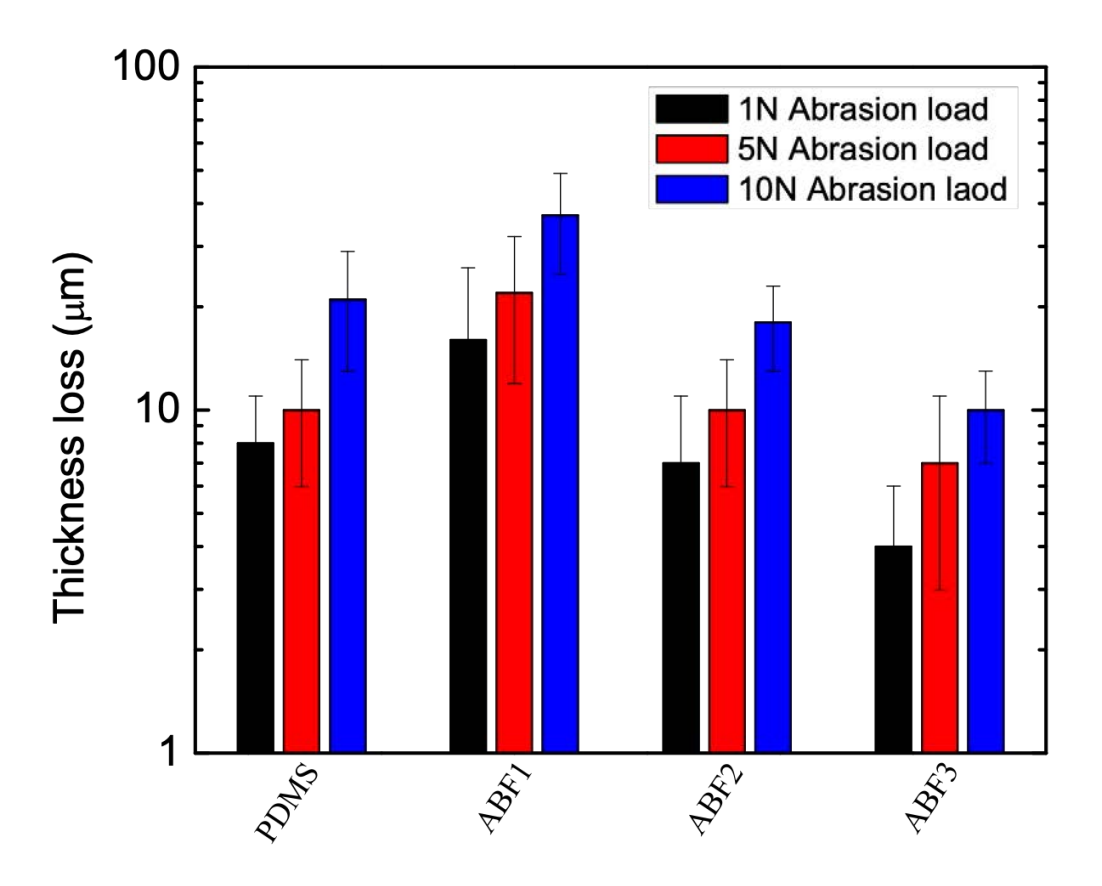


Figure 13. Abrasion test results for ABF coatings and PDMS. Primary thickness of each sample is 300 μm . PDMS sample has considered as the standard sample. ABF 3 with lowest concentration of organogels shows the best mechanical durability.

CONCLUSION

We have implemented the idea of stress-localization to minimize adhesion of bio-species on a

surface and have developed durable anti-biofouling surfaces. As demonstrated, these surfaces are

bio-friendly and have no negative impact on marine environment. In a comprehensive study, we

analyzed performance of these stress-localized surfaces with soft and hard bio-species including

Ulva, bacteria, diatoms, barnacles and mussels. ABF1 sample provides minimal attachment to

diatom, Ulva, barnacle and mussel. The stress-localization effect is maximum for ABF1 sample

(i.e. $(g(\varphi_{II})=0.1)$) and leads to its minimal adhesion to hard bio-species. The performance of

ABF1 is better than state-of-the-art anti-biofouling samples. For anti-bacterial characteristics to

minimize growth, ABF3 is the winner sample in comparison to state-of-the-art and control

samples. Lower concentration of second phase (i.e. organogel) may have contributed to this anti-

bacterial characteristic. Stress-localized coatings provide less suitable environment for

attachment of marine fouling organisms and allows to minimize adhesion of hard objects on a

surface with no compromise in durability of these coatings.

AUTHOR INFORMATION

Corresponding Author

*E-mail: hghasemi@uh.edu

Author Contributions

H. G. conceived the idea. B. E. and P. I. developed the surfaces. B. E. and S. S. conducted the

experiments. P. J. and M. N. conducted the surface durability experiments. A. M. and V. K.

helped on SPM characterization experiments. B. E. and H. G. wrote the manuscript and all the

authors commented on the manuscript. H. G. directed the research.

Notes

24

The authors declare no competing financial interest.

ACKNOWLEDGMENT

The authors gratefully acknowledge funding support from the Office of Naval Research (ONR) for grant N00014-17-1-2978 with Dr. Paul Armistead and Dr. Kathryn J. Wahl as program managers.

References

- (1) Callow, J. a; Callow, M. E. Trends in the Development of Environmentally Friendly Fouling-Resistant Marine Coatings. *Nat. Commun.* **2011**, *2*, 244.
- (2) Terlizzi, A.; Fraschetti, S.; Gianguzza, P.; Faimali, M.; Boero, F. En 7 Ironmental Impact of Antifouling Technologies: State of the Art and Perspecti 7 Es. **2001**, *317*, 311–317.
- (3) Yebra, D. M.; Kiil, S.; Dam-Johansen, K. Antifouling Technology Past, Present and Future Steps towards Efficient and Environmentally Friendly Antifouling Coatings. *Prog. Org. Coatings* **2004**, *50*, 75–104.
- (4) Kirschner, C. M.; Brennan, A. B. Bio-Inspired Antifouling Strategies. *Annu. Rev. Mater. Res.* **2012**, *42*, 211–229.
- (5) Chambers, L. D.; Stokes, K. R.; Walsh, F. C.; Wood, R. J. K. Modern Approaches to Marine Antifouling Coatings. *Surf. Coatings Technol.* **2006**, *201*, 3642–3652.
- (6) Schultz, M.; Bendick, J.; Holm, E.; Hertel, W. Economic Impact of Biofouling on a Naval Surface Ship. *Biofouling* **2011**, *27*, 87–98.
- (7) Dürr, S.; Thomason, J. C. *Biofouling*, 1st ed.; WILEY-BLACKWELL: Chichester, 2010.
- (8) Videla, H. A. *Manual of Biocorrosion*, 1st ed.; McCombs, K., Ed.; CRS Press: Boca Raton, 1996.
- (9) Lejars, M.; Margaillan, A.; Bressy, C. Fouling Release Coatings: A Nontoxic Alternative to Biocidal Antifouling Coatings. *Chem. Rev.* **2012**, *112*, 4347–4390.
- (10) J.A. Callow, M. E. C. Antifouling Compounds; Springer, Berlin, Heidelberg, 2006.
- (11) Patel, P.; Callow, M. E.; Joint, I.; Callow, J. A. Specificity in the Settlement Modifying Response of Bacterial Biofilms towards Zoospores of the Marine Alga Enteromorpha. *Environ. Microbiol.* **2003**, *5*, 338–349.
- (12) Costerton, J. W. Introdution to Biofilm. Int. J. Antimicrob. Agents 1999, 11, 217–221.
- (13) Jain, A.; Bhosle, N. B. Biochemical Composition of the Marine Conditioning Film: Implications for Bacterial Adhesion. *Biofouling* **2009**, *25*, 13–19.

- (14) Abarzua, S.; Jakubowski, S. Biotechnological Investigation for the Prevention of Biofouling. 1. Biological and Biochemical Principles for the Prevention of Biofouling. *Mar. Ecol. Prog. Ser.* **1995**, *123*, 301.
- (15) Qian, P. Y.; Lau, S. C. K.; Dahms, H. U.; Dobretsov, S.; Harder, T. Marine Biofilms as Mediators of Colonization by Marine Macroorganisms: Implications for Antifouling and Aquaculture. *Mar. Biotechnol.* **2007**, *9*, 399–410.
- (16) Haras, D. Biofilms and Deteriorations of Materials: From Analysis of the Phenomenon to Prevention Strategies. *Mater. Tech.* **2005**, *93*, 27–41.
- (17) Sheng, G.; Yu, H.; Li, X. Extracellular Polymeric Substances (EPS) of Microbial Aggregates in Biological Wastewater Treatment Systems: A Review. **2010**, *28*, 882–894.
- (18) Lin, H.; Zhang, M.; Wang, F.; Meng, F.; Liao, B. Q.; Hong, H.; Chen, J.; Gao, W. A Critical Review of Extracellular Polymeric Substances (EPSs) in Membrane Bioreactors: Characteristics, Roles in Membrane Fouling and Control Strategies. *J. Memb. Sci.* **2014**, *460*, 110–125.
- (19) Schumacher, J. F.; Aldred, N.; Callow, M. E.; Finlay, J. A.; Callow, J. A.; Clare, A. S.; Brennan, A. B. Species-Specific Engineered Antifouling Topographies: Correlations between the Settlement of Algal Zoospores and Barnacle Cyprids. *Biofouling* **2007**, *23*, 307–317.
- (20) Berntsson, K. M.; Jonsson, P. R.; Lejhall, M.; Gatenholm, P. Analysis of Behavioural Rejection of Micro-Textured Surfaces and Implications for Recruitment by the Barnacle Balanus Improvisus. *J. Exp. Mar. Bio. Ecol.* **2000**, *251*, 59–83.
- (21) Fletcher, R. L.; Callow, M. E. The Settlement, Attachment and Establishment of Marine Algal Spores. *Br. Phycol. J.* **1992**, *27*, 303–329.
- (22) Callow, M. E.; Fletcher, R. L. The Influence of Low Surface Energy Materials on Bioadhesion-a Review. *Int. Biodeterior. Biodegradation* **1994**, *34*, 333–348.
- (23) Liu, Y.; Zhao, Q. Influence of Surface Energy of Modified Surfaces on Bacterial Adhesion. *Biophys. Chem.* **2005**, *117*, 39–45.
- (24) Brady, R. F.; Singer, I. L. Mechanical Factors Favoring Release from Fouling Release Coatings. *Biofouling* **2000**, *15*, 73–81.
- (25) Sun, Y.; Guo, S.; Walker, G. C.; Kavanagh, C. J.; Swain, G. W. Surface Elastic Modulus of Barnacle Adhesive and Release Characteristics from Silicone Surfaces. *Biofouling* **2004**, *20*, 279–289.
- (26) Champ, M. a. The Status of the Treaty to Ban TBT in Marine Antifouling Paints and Alternatives. *Proc. 24th UJNR Mar. Facil. Panel Meet.* **2001**, 1–7.
- (27) Champ, M. A. A Review of Organotin Regulatory Strategies, Pending Actions, Related Costs and Benefits. *Sci. Total Environ.* **2000**, *258*, 21–71.

- (28) Strand, J.; Jacobsen, J. A. Accumulation and Trophic Transfer of Organotins in a Marine Food Web from the Danish Coastal Waters. *Sci. Total Environ.* **2005**, *350*, 72–85.
- (29) Evans, S. M.; Leksono, T.; McKinnell, P. D. Tributyltin Pollution: A Diminishing Problem Following Legislation Limiting the Use of TBT-Based Anti-Fouling Paints. *Mar. Pollut. Bull.* **1995**, *30*, 14–21.
- (30) Terlizzi, A.; Fraschetti, S.; Gianguzza, P.; Faimali, M.; Boero, F. Environmental Impact of Antifouling Technologies: State of the Art and Perspectives. *Aquat. Conserv. Mar. Freshw. Ecosyst.* **2001**, *317*, 311–317.
- (31) Alzieu, C. Environmental Impact of TBT: The French Experience. *Sci. Total Environ.* **2000**, *258*, 99–102.
- (32) Krishnan, S.; Weinman, C. J.; Ober, C. K. Advances in Polymers for Anti-Biofouling Surfaces. *J. Mater. Chem.* **2008**, *18*, 3405.
- (33) Schmidt, D. L.; Brady, R. F.; Lam, K.; Schmidt, D. C.; Chaudhury, M. K. Contact Angle Hysteresis, Adhesion, and Marine Biofouling. *Langmuir* **2004**, *20*, 2830–2836.
- (34) Donald L. Schmidt, Charles E. Coburn, Benjamin M. DeKoven, Gregg E. Potter, Gregory F. Meyers, A. D. A. F. Water-Based Non-Stick Hydrophobic Coatings. *Nature* **1994**, *368*, 39–41.
- (35) Qiu, H.; Hölken, I.; Gapeeva, A.; Filiz, V.; Adelung, R.; Baum, M. Development and Characterization of Mechanically Durable Silicone-Polythiourethane Composites Modified with Tetrapodal Shaped ZnO Particles for the Potential Application as Fouling-Release Coating in the Marine Sector.
- (36) Wang, Y.; Yao, X.; Wu, S.; Li, Q.; Lv, J.; Wang, J. Bioinspired Solid Organogel Materials with a Regenerable Sacrificial Alkane Surface Layer. **2017**, *1700865*, 1–7.
- (37) Lv, J.; Yao, X.; Zheng, Y.; Wang, J.; Jiang, L. Antiadhesion Organogel Materials: From Liquid to Solid. **2017**, *1703032*, 1–8.
- (38) Ekblad, T.; Bergstro, G.; Ederth, T.; Conlan, S. L.; Mutton, R.; Clare, A. S.; Wang, S.; Liu, Y.; Zhao, Q.; Souza, F. D.; Donnelly, G. T.; Willemsen, R.; Pettitt, M. E.; Callow, M. E.; Callow, J. a; Liedberg, B. Poly (Ethylene Glycol) -Containing Hydrogel Surfaces for Antifouling Applications in Marine and Freshwater Environments Poly (Ethylene Glycol) -Containing Hydrogel Surfaces for Antifouling Applications in Marine and Freshwater Environments. 2008, 2775–2783.
- (39) Galhenage, T. P.; Webster, D. C.; Moreira, A. M. S.; Burgett, R. J.; Stafslien, S. J.; Vanderwal, L.; Finlay, J. A.; Franco, S. C.; Clare, A. S. Polyurethane Coatings and Their Performance as Fouling-Release Surfaces. *J. Coatings Technol. Res.* **2017**, *14*, 307–322.
- (40) Amini, S.; Kolle, S.; Petrone, L.; Ahanotu, O.; Sunny, S.; Sutanto, C. N.; Hoon, S.; Cohen, L.; Weaver, J. C.; Aizenberg, J.; Vogel, N.; Miserez, A. Preventing Mussel Adhesion Using Lubricant-Infused Materials. *Science* (80-.). 2017, 357, 668–673.

- (41) Xiao, L.; Li, J.; Mieszkin, S.; Di Fino, A.; Clare, A. S.; Callow, M. E.; Callow, J. A.; Grunze, M.; Rosenhahn, A.; Levkin, P. A. Slippery Liquid-Infused Porous Surfaces Showing Marine Antibiofouling Properties. *ACS Appl. Mater. Interfaces* **2013**, *5*, 10074–10080.
- (42) Masoudi, A.; Irajizad, P.; Farokhnia, N.; Kashyap, V.; Ghasemi, H. Antiscaling Magnetic Slippery Surfaces. *ACS Appl. Mater. Interfaces* **2017**, *9*, 21025–21033.
- (43) Epstein, A. K.; Wong, T.-S.; Belisle, R. A.; Boggs, E. M.; Aizenberg, J. Liquid-Infused Structured Surfaces with Exceptional Anti-Biofouling Performance. *Proc. Natl. Acad. Sci.* **2012**, *109*, 13182–13187.
- (44) Nurioglu, A. G.; Esteves, A. C. C.; De With, G. Non-Toxic, Non-Biocide-Release Antifouling Coatings Based on Molecular Structure Design for Marine Applications. *J. Mater. Chem. B* **2015**, *3*, 6547–6570.
- (45) Xing, C.; Meng, F.; Quan, M.; Ding, K.; Dang, Y.; Gong, Y. Acta Biomaterialia Quantitative Fabrication, Performance Optimization and Comparison of PEG and Zwitterionic Polymer Antifouling Coatings. *Acta Biomater.* **2017**, *59*, 129–138.
- (46) Yeh, S.; Chen, C.; Chen, W.; Huang, C. Modi Fi Cation of Silicone Elastomer with Zwitterionic Silane for Durable Antifouling Properties. **2014**.
- (47) Leng, C.; Hung, H.; Sieggreen, O. A.; Li, Y.; Jiang, S.; Chen, Z. Probing the Surface Hydration of Nonfouling Zwitterionic and Poly(Ethylene Glycol) Materials with Isotopic Dilution Spectroscopy. **2015**, 1–6.
- (48) Zhang, L.; Cao, Z.; Bai, T.; Carr, L.; Irvin, C.; Ratner, B. D.; Jiang, S. Letters Zwitterionic Hydrogels Implanted in Mice Resist the Foreign-Body Reaction. **2013**, *31*.
- (49) Xie, Q.; Liu, C.; Zhang, G. Poly(Dimethylsiloxane)-Based Polyurethane with Chemically Attached Antifoulants for Durable Marine Antibiofouling. **2015**.
- (50) Zhang, H.; Chiao, M. Anti-Fouling Coatings of Poly (Dimethylsiloxane) Devices for Biological and Biomedical Applications. *J. Med. Biol. Eng.* **2015**, 143–155.
- (51) Scardino, A. J.; Nys, R. de. Mini Review: Biomimetic Models and Bioinspired Surfaces for Fouling Control. *Biofouling* **2011**, *27*, 73–86.
- (52) Bohn, H. F.; Federle, W. Insect Aquaplaning: Nepenthes Pitcher Plants Capture Prey with the Peristome, a Fully Wettable Water-Lubricated Anisotropic Surface. *Proc. Natl. Acad. Sci. U. S. A.* **2004**, *101*, 14138–14143.
- (53) Wong, T.-S.; Kang, S. H.; Tang, S. K. Y.; Smythe, E. J.; Hatton, B. D.; Grinthal, A.; Aizenberg, J. Bioinspired Self-Repairing Slippery Surfaces with Pressure-Stable Omniphobicity. *Nature* **2011**, *477*, 443–447.
- (54) Irajizad, P.; Al-Bayati, A.; Eslami, B.; Shafquat, T.; Nazari, M.; Jafari, P.; Kashyap, V.; Masoudi, A.; Araya, D.; Ghasemi, H. Stress-Localized Durable Icephobic Surfaces. *Mater. Horizons* **2019**, *6*, 758–766.

- (55) Chaudhury, M. K.; Kim, K. H. Shear-Induced Adhesive Failure of a Rigid Slab in Contact with a Thin Confined Film. *Eur. Phys. J. E* **2007**, *23*, 175–183.
- (56) Irajizad, P.; Al-bayati, A.; Eslami, B.; Shafquat, T.; Nazari, M.; Jafari, P.; Kashyap, V.; Masoudi, A.; Araya, D.; Ghasemi, H. Materials Horizons. **2019**, *19*.
- (57) Urata, C.; Dunderdale, G. J.; England, M. W.; Hozumi, A. Self-Lubricating Organogels (SLUGs) with Exceptional Syneresis-Induced Anti-Sticking Properties against Viscous Emulsions and Ices. *J. Mater. Chem. A* **2015**, *3*, 12626–12630.
- (58) Callow, M. E.; Callow, J. A.; Conlan, S.; Clare, A. S.; Stafslien, S. Efficacy Testing of Nonbiocidal and Fouling-Release Coatings. In *Biofouling Methods*; Dobretsov, S., Willimas, D. N., Thomason, J. C., Eds.; Wiley Blackwell: Oxford, 2014; pp 291–316.
- (59) Krishnan, S.; Wang, N.; Ober, C. K.; Finlay, J. A.; Callow, M. E.; Callow, J. A.; Hexemer, A.; Sohn, K. E.; Kramer, E. J.; Fischer, D. A. Comparison of the Fouling Release Properties of Hydrophobic Fluorinated and Hydrophilic PEGylated Block Copolymer Surfaces: Attachment Strength of the Diatom Navicula and the Green Alga Ulva. *Biomacromolecules* **2006**, *7*, 1449–1462.
- (60) Schilp, S.; Kueller, A.; Rosenhahn, A.; Grunze, M.; Pettitt, M. E.; Callow, M. E.; Callow, J. A. Settlement and Adhesion of Algal Cells to Hexa(Ethylene Glycol)-Containing Self-Assembled Monolayers with Systematically Changed Wetting Properties. *Biointerphases* 2007, 2, 143–150.
- (61) Walker, G. C.; Sun, Y.; Guo, S.; Finlay, J. A.; Callow, M. E.; Callow, J. A. Surface Mechanical Properties of the Spore Adhesive of the Green Alga *Ulva. J. Adhes.* **2005**, *81*, 1101–1118.
- (62) Schilp, S.; Rosenhahn, A.; Pettitt, M. E.; Bowen, J.; Callow, M. E.; Callow, J. A.; Grunze, M. Physicochemical Properties of (Ethylene Glycol)-Containing Self-Assembled Monolayers Relevant for Protein and Algal Cell Resistance. *Langmuir* 2009, 25, 10077–10082.
- (63) Jiang, Y.; Turner, K. T. Measurement of the Strength and Range of Adhesion Using Atomic Force Microscopy. *Extrem. Mech. Lett.* **2016**, *9*, 119–126.
- (64) Reads, C. The Influence of Elastic Modulus and Thickness on the Release of the Soft-Fouling Green Alga Ulva Linza (Syn . Enteromorpha ... **2015**.
- (65) Ekin, A.; Webster, D. C.; Daniels, J. W.; Stafslien, S. J.; Cassé, F.; Callow, J. A.; Callow, M. E. Synthesis, Formulation, and Characterization of Siloxane-Polyurethane Coatings for Underwater Marine Applications Using Combinatorial High-Throughput Experimentation. *J. Coatings Technol. Res.* 2007, 4, 435–451.
- (66) Molino, P. J.; Wetherbee, R. The Biology of Biofouling Diatoms and Their Role in the Development of Microbial Slimes. *Biofouling* **2008**, *24*, 365–379.
- (67) Holland, R.; Dugdale, T. M.; Wetherbee, R.; Brennan, a B.; Finlay, J. a; Callow, J. a; Callow, M. E. Adhesion and Motility of Fouling Diatoms on a Silicone Elastomer.

- Biofouling 2004, 20, 323-329.
- (68) Flemming, H.-C. C.; Wingender, J. Relevance of Microbial Extracellular Polymeric Substances (EPSs)--Part II: Technical Aspects. *Water Sci. Technol.* **2001**, *43*, 9–16.
- (69) Liu, Y.; Fang, H. H. P. Influences of Extracellular Polymeric Substances (EPS) on Flocculation, Settling, and Dewatering of Activated Sludge. *Crit. Rev. Environ. Sci. Technol.* **2003**, *33*, 237–273.
- (70) Boyle, J. A.; Pickett-Heaps, J. D.; Czarnecki, D. B. Valve Morphogenesis in the Pennate Diatom Achnanthes Coarctata. *J. Phycol.* **1984**, *20*, 563–573.
- (71) Mayer, C.; Moritz, R.; Kirschner, C.; Borchard, W.; Maibaum, R.; Wingender, J.; Flemming, H. The Role of Intermolecular Interactions: Studies on Model Systems for Bacterial Biofilms. **1999**, *26*, 3–16.
- (72) Sheng, G. P.; Yu, H. Q.; Li, X. Y. Extracellular Polymeric Substances (EPS) of Microbial Aggregates in Biological Wastewater Treatment Systems: A Review. *Biotechnol. Adv.* **2010**, *28*, 882–894.
- (73) Hamm, C. E.; Merkel, R.; Springer, O.; Jurkojc, P.; Maiert, C.; Prechtelt, K.; Smetacek, V. Architecture and Material Properties of Diatom Shells Provide Effective Mechanical Protection. *Nature* **2003**, *421*, 841–843.
- (74) Coombs, J.; Darley, W. M.; Holm-Hansen, O.; Volcani, B. E. Studies on the Biochemistry and Fine Structure of Silica Shell Formation in Diatoms. Photosynthesis and Respiration in Silicon-Starvation Synchrony. *Plant Physiol.* **1967**, *42*, 1607–1611.
- (75) Dickinson, G. H.; Vega, I. E.; Wahl, K. J.; Orihuela, B.; Beyley, V.; Rodriguez, E. N.; Everett, R. K.; Bonaventura, J.; Rittschof, D. Barnacle Cement: A Polymerization Model Based on Evolutionary Concepts. *J. Exp. Biol.* **2009**, *212*, 3499–3510.
- (76) Barlow, D. E.; Dickinson, G. H.; Orihuela, B.; Kulp, J. L.; Rittschof, D.; Wahl, K. J. Characterization of the Adhesive Plaque of the Barnacle Balanus Amphitrite: Amyloid-like Nanofibrils Are a Major Component. *Langmuir* **2010**, *26*, 6549–6556.
- (77) Wiegemann, M. Adhesion in Blue Mussels (Mytilus Edulis) and Barnacles (Genus Balanus): Mechanisms and Technical Applications. *Aquat. Sci.* **2005**, *67*, 166–176.
- (78) Kamino, K.; Inoue, K.; Maruyama, T.; Takamatsu, N.; Harayama, S.; Shizuri, Y. Barnacle Cement Proteins: Importance of Disulfide Bonds in Their Insolubility. *J. Biol. Chem.* **2000**, *275*, 27360–27365.
- (79) Waite, J. H. Nature's Underwater Adhesive Specialist. *Int. J. Adhes. Adhes.* **1987**, 7, 9–14.
- (80) Yu, J.; Kan, Y.; Rapp, M.; Danner, E.; Wei, W.; Das, S.; Miller, D. R.; Chen, Y.; Waite, J. H.; Israelachvili, J. N. Adaptive Hydrophobic and Hydrophilic Interactions of Mussel Foot Proteins with Organic Thin Films. *Proc. Natl. Acad. Sci.* **2013**, *110*, 15680–15685.
- (81) Lee, B. P.; Messersmith, P. B.; Israelachvili, J. N.; Waite, J. H. Mussel-Inspired

Adhesives and Coatings. Annu. Rev. Mater. Res. 2011, 41, 99–132.